Original Article

Chemical exchange saturation transfer (CEST) magnetic resonance imaging (MRI) quantification of transient ischemia using a combination method of 5-pool Lorentzian fitting and inverse Z-spectrum analysis

Lihong Zhang[1], Chongxin Xu[1], Zhen Li[2], Junding Sun[1]^, Xiaoli Wang[2], Beibei Hou[1], Yingcheng Zhao[3]

[1]College of Computer Science and Technology, Henan Polytechnic University, Jiaozuo, China; [2]Department of Medical Imaging, Weifang Medical University, Weifang, China; [3]Xi'an Key Lab of Radiomics and Intelligent Perception, School of Information Sciences and Technology, Northwest University, Xi'an, China

Contributions: (I) Conception and design: L Zhang; (II) Administrative support: J Sun, X Wang; (III) Provision of study materials or patients: X Wang, Z Li; (IV) Collection and assembly of data: L Zhang, C Xu, J Sun, Z Li, X Wang, Y Zhao; (V) Data analysis and interpretation: L Zhang; (VI) Manuscript writing: All authors; (VII) Final approval of manuscript: All authors.

Correspondence to: Junding Sun. College of Computer Science and Technology, Henan Polytechnic University, 2001 Century Avenue, Jiaozuo 454003, China. Email: sunjd@hpu.edu.cn; Xiaoli Wang. Department of Medical Imaging, Weifang Medical University, No. 7166, Baotong West Street, Weifang 261053, China. Email: wxlpine@163.com.

Background: Chemical exchange saturation transfer (CEST) is a promising method for the detection of biochemical alterations in cancers and neurological diseases. However, the sensitivity of the currently existing quantitative method for detecting ischemia needs further improvement.

Methods: To further improve the quantification of the CEST signal and enhance the CEST detection for ischemia, we used a quantitative analysis method that combines an inverse Z-spectrum analysis and a 5-pool Lorentzian fitting. Specifically, a 5-pool Lorentzian simulation was conducted with the following brain tissue parameters: water, amide (3.5 ppm), amine (2.2 ppm), magnetization transfer (MT), and nuclear Overhauser enhancement (NOE; –3.5 ppm). The parameters were first calculated offline and stored as the initial value of the Z-spectrum fitting. Then, the measured Z-spectrum with the peak value set to 0 was fitted via the stored initial value, which yielded the reference Z-spectrum. Finally, the difference between the inverse of the Z-spectrum and the inverse of the reference Z-spectrum was used as the CEST definite spectrum.

Results: The simulation results demonstrated that the Z-spectra of the rat brain were well simulated by a 5-pool Lorentzian fitting. Further, the proposed method detected a larger difference than did either the saturation transfer difference or the 5-pool Lorentzian fitting, as demonstrated by simulations. According to the results of the cerebral ischemia rat model, the proposed method provided the highest contrast-to-noise ratio (CNR) between the contralateral and the ipsilateral striatum under various acquisition conditions. The results indicated that the difference of fitted amplitudes generated with a 5-pool Lorentzian fitting in amide at 3.5 ppm (6.04%±0.39%; 6.86%±0.39%) was decreased in a stroke lesion compared to the contralateral normal tissue. Moreover, the difference of the residual of inversed Z-spectra in which 5-pool Lorentzian fitting was used to calculate the reference Z-spectra (MTR_{Rex}^{5L}) amplitudes in amide at 3.5 ppm (13.83%±2.20%, 15.69%±1.99%) was reduced in a stroke lesion compared to the contralateral normal tissue.

Conclusions: MTR_{Rex}^{5L} is predominantly pH-sensitive and is suitable for detecting tissue acidosis following an acute stroke.

^ ORCID: 0000-0001-7349-0248.

Keywords: Chemical exchange saturation transfer (CEST); acute stroke; magnetization transfer ratio yielding rex (MTR_{Rex}); 5-pool Lorentzian fitting

Submitted Apr 27, 2022. Accepted for publication Oct 30, 2022. Published online Dec 05, 2022.
doi: 10.21037/qims-22-420
View this article at: https://dx.doi.org/10.21037/qims-22-420

Introduction

Due to insufficient blood supply, ischemic brain tissue first experience changes in oxygen and glucose metabolism during a stroke. This leads to a decrease in the acidic microenvironment; that is, a decrease in the pH value. The chemical exchange saturation transfer (CEST) peak of the amide proton in ischemic cerebral tissue is lower than the peak in normal tissue (1). The classic definition of the ischemic penumbra is the area of tissue surrounding the ischemic core that is subject to abnormal perfusion and metabolism (2). The current clinical treatment only aims at the ischemic penumbra and has no therapeutic effect on the infarct area (3). It is possible to salvage tissue from acidosis after proper therapeutic interventions and reperfusion. Accordingly, finding imaging tools to accurately and promptly identify reversibly damaged tissue in the ischemic penumbra can assist in clinical decision-making and allow quick therapeutic interventions for improved outcomes.

Magnetic resonance spectroscopy (MRS) has been used to assess tissue pH values during stroke (4). However, its practical applicability is limited due to its low spatial and temporal resolutions (5). CEST offers a novel type of magnetic resonance imaging (MRI) contrast mechanism (6). CEST has received substantial attention in recent years because of its potential to detect low-concentration proteins and metabolites *in vivo* (7). In chemical exchange saturation transfer magnetic resonance imaging (CEST-MRI), pH-weighted imaging has significantly higher pH sensitivity than do the conventional MRS techniques (8). Accordingly, this technique has been successfully used for the quantitative evaluation of dilute metabolites and pH values in metabolic disorders, such as stroke, in both preclinical (9-12) and clinical studies (13). In addition to predicting stroke outcomes, CEST provides additional metabolic information to differentiate between benign oligomers and metabolic penumbra.

In previous amide proton transfer (APT) research, comparatively easy, relatively simple measurements of asymmetry analysis magnetization transfer ratio based on asymmetry (MTR_{asym}) have been used for quantification (1). However, MTR_{asym} may be interfered with by nuclear Overhauser enhancement (NOE) and semisolid macromolecular magnetization transfer (MT) (14,15). Recently, other methods for analyzing CEST data have been introduced, including Lorentzian difference (LD) (16), three-offsets (17), multiple-pool Lorentzian fitting (18-21), and spillover-corrected magnetization transfer ratio yielding rex (MTR_{Rex}) (11). A recent comparison study indicated that the multiple-pool Lorentzian fitting method can provide more accurate quantitative CEST and NOE effects than can LD and three-offsets, particularly at low irradiation powers (22). A voxel-wise optimization of the pseudo-Voigt profile (VOPVP) fitting algorithm has been reported, which uses a linear combination of Lorentzian and Gaussian functions as the reference spectra to improve the deficiencies of traditional LD analysis (15). Furthermore, it has been shown that the effects add up inversely to the Z-spectrum; therefore, an inverse Z transform was used to detect an ischemic stroke (11). Recently, a proposed method MTR_{Rex}^{VOPVP} was used to determine the residual between the inverse experimental Z-spectra and the reference Z-spectra calculated by VOPVP methods (12). This method was proven to enhance the CEST detection for ischemia. However, which parameters may be used as a marker for detection of an acute ischemic stroke at an early stage has not yet been elucidated. Therefore, it is essential to identify these parameters to further improve pH value quantification.

Previous study also showed that a down-sampling expedited adaptive least-squares fitting could effectively quantify multi-pool contributions in adult male Wistar rats both before and after global cerebral ischemia (18). However, compared with the dip from the CEST signal of normal brain tissue, the dip from the CEST signal 2 hours after a transient ischemia caused through middle cerebral artery occlusion (MCAO) becomes less obvious. Research suggests that a novel NOE-mediated MT signal around –1.6 ppm could be identified credibly in rat brains through a method that combines a multi-pool Lorentzian fitting and an inverse, while the dip is not simply detected from the

Z-spectrum directly (23).

In this work, a novel method using a combination of an inverse Z-spectrum analysis and a 5-pool Lorentzian fitting named MTR_{Rex}^{5L} is proposed. The effectiveness of MTR_{Rex}^{5L} was quantitatively compared to the detection of slight changes that occur in the early stage of stroke through CEST-MRI. In addition, the parameters that could be used as a marker for the detection of an acute ischemic stroke at early stage were identified. The method was validated by a well-established animal model.

Methods

Theory

CEST-MRI usually involves a range of images with saturation pulse sweeping through a series of frequency offsets, collecting offset changes with the signal, also known as the Z-spectra (24). Fitting individual contributors to the Z-spectrum may increase the accuracy the quantification of each component (22). MTR_{Rex}^{5L} completes the fitting in two steps. First, to eliminate the background MT and direct water saturation (DS) effects, a 5-pool Lorentzian fitting of Z-spectra through a nonlinear optimization algorithm is performed (25). The model of the 5-pool Lorentzian fitting method is shown in Eq. [1] and Eq. [2].

$$S(\Delta\omega) = 1 - \sum_{i=1}^{5} L_i(\Delta\omega) \quad [1]$$

$$L_i(\Delta\omega) = A_i \frac{\Gamma_i^2/4}{\Gamma_i^2/4 + (\Delta\omega - \delta_i)^2} \quad [2]$$

$$Z_{ref,j}(\Delta\omega) = 1 - \sum_{i\neq j}^{n=5} L_i(\Delta\omega) \quad [3]$$

$$Z_{residual}^{5L}(\delta_i) = Z_{ref,i}(\delta_i) - Z_{exp}(\delta_i) \quad [4]$$

Here, A_i, Γ_i, and δ_i represent the peak amplitude, peak full width at half maximum, and a Lorentzian line with a central frequency offset from the water of each pool, respectively. The CEST residual spectra (as shown by Eq. [4]) is gained using a subtraction of the reference Z-spectra ($Z_{ref,i}$, as defined by Eq. [3]), which consists of each Lorentzian (except that of pool *i*), from the Z-spectra of the experiment (Z_{exp}). All starting points and boundaries of the fitting parameters for the rodent brain tissue of the 5-pool Lorentzian fitting are presented in *Table 1* (19).

Furthermore, it has been shown that the effects add up inversely to the Z-spectrum (11,19,26). To provide a more specific quantification, the fitted spectra were treated as a reference signal ($Z_{ref,i}$), which represented the background DS and the semisolid MT effects. This reference signal was subtracted as an inverse transform from the complete fitting of the Z-spectra (Z_{exp}), which yielded MTR_{Rex}^{5L} (23) (as defined by Eq. [5]):

$$MTR_{Rex}^{5L}(\Delta\omega) = \frac{1}{Z_{exp}(\delta_i)} - \frac{1}{Z_{ref,i}(\delta_i)} \quad [5]$$

After this first round of fitting, two peaks of NOE and CEST close to –3.6, 2, and 3.5 ppm were solved by a secondary fitting.

Specifically, R_{ex}^{cest} is independent of nonspecific tissue parameters (e.g., DS, T_{1w} and semisolid MT effects), and depends only on the solute concentration (f_s), solute transverse relaxation (R_{2s}), solute–water exchange rate (k_{sw}), and irradiation power , as shown in Eq. [6] (22):

$$R_{ex}^{cest}(\Delta\omega) = \frac{f_s k_{sw} \omega_1^2}{\omega_1^2 + (R_{2s} + k_{sw}) k_{sw} + (\Delta\omega - \Delta)^2 k_{sw} / (R_{2s} + k_{sw})} \quad [6]$$

The MTR_{Rex} was given by Zaiss *et al.* using the 1/Z analysis, as defined by Eq. [7] (11):

$$MTR_{Rex}(3.5ppm) = \left(\frac{1}{Z_{lab}} - \frac{1}{Z_{ref}}\right) = \left(\frac{1}{Z(3.5ppm)} - \frac{1}{Z(-3.5ppm)}\right) \quad [7]$$

Specifically, the quantification was obtained as shown in Eq. [8] (12),

$$MTR_{Rex}^{VOPVP}(\Delta\omega) = \frac{S_0}{S_{exp}(\Delta\omega)} - \frac{S_0}{S_{ref}(\Delta\omega)} \quad [8]$$

where $S_{ref}(\Delta\omega)/S_0$ is the reference Z-spectra (as evaluated by fitting the experimental Z-spectra using the anterior reported VOPVP) (15), and $S_{exp}(\Delta\omega)/S_0$ is mean the experimental Z-spectra.

The obtained data were evaluated using the contrast-to-noise ratio (CNR) (18), as shown in Eq. [9]:

$$CNR = \frac{|S_1 - S_2|}{\sqrt{(\sigma_1^2 + \sigma_2^2)}} \quad [9]$$

where S_1 and S_2 are are the mean values for the 2 regions of interest (ROIs), respectively. δ_1 and δ_2 are their standard deviations, respectively.

Simulation

The Z-spectrum of rat brain are determined using the tissue parameters listed in *Table 1* (1,12,25). Numerical simulations were performed to evaluate the specificity of the parameters. The simulations had different exchange rates

Table 1 Parameters for the 5-pool numerical simulation: solute concentration (f_s), solute-water exchange rate (k_{sw}), longitudinal relaxation time (T_1), transverse relaxation time (T_2), and solute frequency offset (Δ)

Parameter	Water	Amide	Amine	NOE	MT
f_s	1	0.004	0.002	0.0033	0.04
k_{sw} (s^{-1})	–	30 (contralateral), 18 (ipsilateral striatum)	1,000	20	20
T_1 (s)	2	2	3	2	2
T_2 (ms)	60	38	38	0.4	20×10^{-3}
Δ (ppm)	0	3.5	2	–3.6	0

NOE, nuclear Overhauser enhancement, MT, magnetization transfer.

and measurements of tissue homogenates with different pH values.

Animals

This study was approved by the ethics board of Weifang Medical University, which conforms to the institutional guidelines for the care and use of animals. Transient focal cerebral ischemia occurred in 5 adult male Sprague-Dawley rats weighing 240 to 270 g, as reported previously (12). The rats experienced MCAO for 2 hours via an intraluminal suture (27). A 4-0 nylon monofilament suture with a tip surrounded by wax entered the lumen from the external carotid artery until the suture was inserted into the internal carotid artery, blocking the bifurcation of the anterior and middle cerebral arteries. Two hours after the MCAO, the nylon suture was drawn out for reperfusion. Throughout the experiments, the body temperature of the animals was monitored and maintained at 37±0.5 ℃. Age- and sex-matched rats were used as normal controls (n=5). The animals were anesthetized with 2–98% isoflurane for induction and surgery, and 2% for maintenance.

MRI scanning

The MRI scans were collected from a 7 Tesla horizontal hole scanner with a diameter of 40 mm (Biospec, Bruker, Billerica, MA, USA) using a transmit-receiver volume coil. After obtaining the T_2-weighted images for multiple slices, the coronal slice at the center of the striatum was scanned with the CEST-MRI. These scans used a continuous wave presaturation pulse with *Tsat* =2,500 ms. This was followed by a fast acquisition with a relaxation enhancement (RARE) readout with repetition time/time to echo (TR/TE) =5,000 ms/4 ms and RARE factor =32. A total of 51 Z-spectrum images with saturation offsets ($\Delta\omega$) in increments between –10 and 10 ppm were obtained ($B_{1\text{-}sat}$ =0.7 and 1 μT), while a total of 35 Z-spectrum images with $\Delta\omega$ increments between –10 and 10 ppm were collected ($B_{1\text{-}sat}$ =2 μT). Moreover, a water saturation shift referencing was collected with $B_{1\text{-}sat}$ =0.5 μT (frequency offsets between ±1 ppm with intervals of 0.1 ppm) (28). For signal normalization, the S_0 of the unsaturated pulse was collected. The apparent diffusion coefficients (ADCs) were acquired by a pulsed gradient spin echo sequence, and the value of *b* was 2,000 s/mm^2. All the images were acquired with a matrix size of 96×64, a field of view of 34×28 mm^2, and a slice thickness 1 mm.

Statistics

The difference between the two groups was evaluated using the *t* test. All data and statistical analyses were calculated by MATLAB R2018 (MathWorks, Natick, MA, USA).

Results

Simulations

The simulations tested whether a 5-pool Lorentzian fitting could accurately describe the real Z-spectrum shape. To simulate the ischemic microenvironment, the simulations were carried out at two different exchange rate levels, which represented different pH values (*Figure 1*). The tissue parameters are listed in *Table 1*. The simulation code was downloaded from the CEST source (29). *Figure 1* shows that the Z-spectra simulated by a 5-pool Lorentzian fitting were very similar to those of the *in vivo* acquisition. However, there was still an obvious difference at approximately –2 ppm between the Z-spectrum of simulation and the results from the *in vivo* acquisition.

To evaluate the performance of the proposed MTR_{Rex}^{5L}

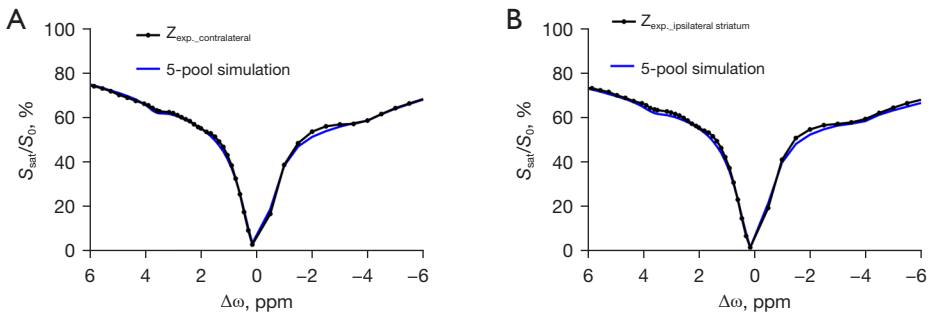

Figure 1 The Z-spectra of an experimental rat brain and simulated results using a 5-pool Lorentzian fit and RF irradiation powers of 1 μT. (A) Contralateral. (B) Ipsilateral striatum. RF, radio frequency.

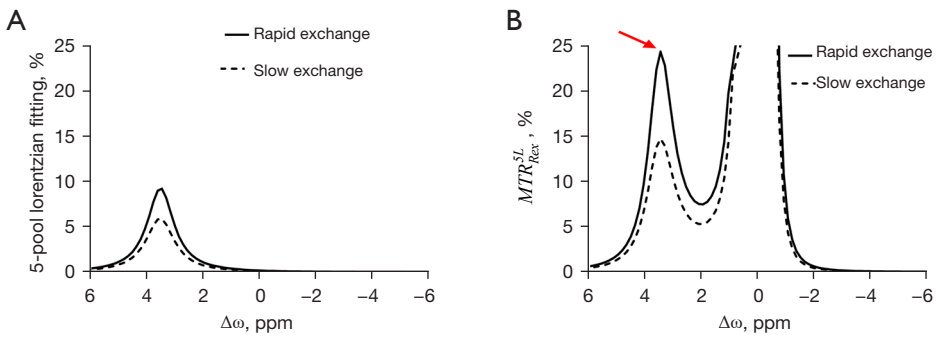

Figure 2 Simulation for 2 different exchange rates of amide and RF irradiation power of 1 μT. (A) A 5-pool Lorentzian fitting. (B) The red arrow indicates the largest signal difference in all the listed methods (solid line, rapid exchange; dashed line, slow exchange; B_{1-sat} =1 μT). RF, radio frequency; MTR_{Rex}, spillover-corrected magnetization transfer ratio yielding rex.

method, a 5-pool model with the tissue parameters from the previous study was used based on the Bloch equation (12). In light of the 2 Z-spectra simulated using the different amide exchange rates, 2 CEST quantification spectra were plotted: 5-pool Lorentzian fit and MTR^{5L}_{Rex} (*Figure 2*). Although MTR^{5L}_{Rex} did not compensate for T1 [as the relaxation enhancement (AREX) did], it exhibited the most obvious difference in the 2 exchange rates among both of the tested quantitative methods. The results were MTR^{5L}_{Rex} =~9.06% and 5-pool Lorentzian fitting =~5.25%, which indicated that MTR^{5L}_{Rex} could more sensitively detect pH changes than could the 5-pool Lorentzian fit (*Figure 2*).

CEST-MRI assessment of stroke rats

Figure 3 demonstrates the ipsilateral striatum and the contralateral using a 5-pool Lorentzian fitting and MTR^{5L}_{Rex} at B_{1-sat} =1 μT, respectively. The starting points and boundaries of the fitting were those used from the previous study (12). The peak amplitude of the amide did not appear to change in the ipsilateral striatum using a 5-pool Lorentzian fitting. Increased amide amplitudes were observed in the contralateral compared with the ipsilateral striatum using MTR^{5L}_{Rex}. The results were in accordance with those of previous studies (12). A decreased NOE amplitude was observed in the contralateral compared with the ipsilateral striatum using a 5-pool Lorentzian fitting and MTR^{5L}_{Rex}. Furthermore, *Figure 3E* compares the original Z-spectra of the ipsilateral striatum and the contralateral. These original Z-spectra were subtracted by the fitted water and MT effects to quantify the CEST effects. Decreased signals were observed in the ipsilateral striatum in comparison to the contralateral. At the same time, apparent peaks were found at 3.5, 2, and –3.5 ppm of the Z-spectra corrected by water and MT. In addition, the ROIs on T_{2w} values are shown in *Figure 3F*—the red lines on the right side represents the stroke lesion, and the green line on the left side represents the contralateral. Similar to other *in vivo* CEST studies (11,30-32). ROIs with similar sizes and shapes were used. Depicting ROIs according to the affected areas needs

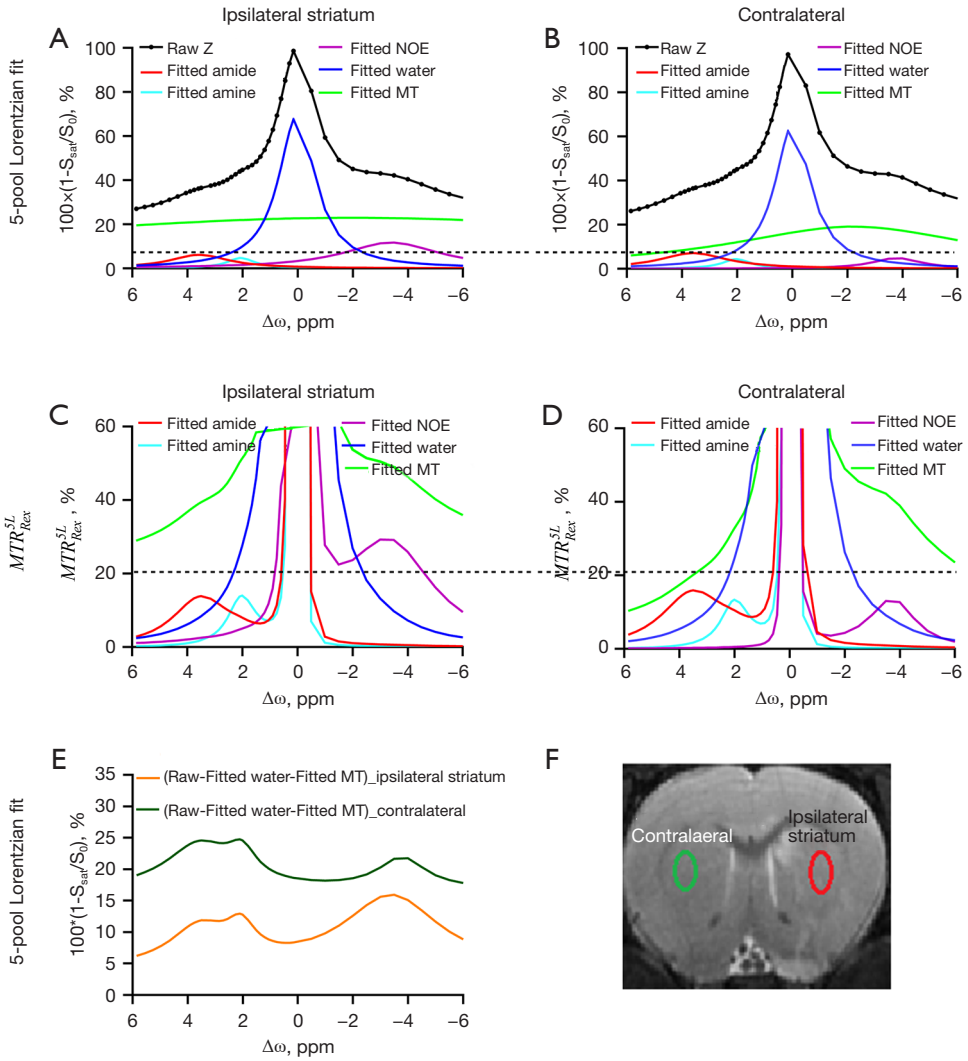

Figure 3 The spectrum analysis between the ipsilateral striatum (left column) and contralateral (right column). (A,B) A 5-pool Lorentzian fitting of Z-spectra from the ipsilateral striatum (left column) and contralateral (right column), including saturation transfer from –3.5, 2, and 3.5 ppm as direct saturation and MT contributions. (C,D) The bottom panels are from the ipsilateral striatum (left column) and contralateral (right column). (E) We subtracted the fitted water and MT effects from the original Z-spectra, showing a clear CEST comparison between normal and ischemic tissues at amide (3.5 ppm) and guanidinium (2 ppm). (F) The T_2-weighted images were labeled as an ipsilateral striatum ROI and the contralateral control for spectral analysis. NOE, nuclear Overhauser enhancement; MT, magnetization transfer; CEST, chemical exchange saturation transfer; ROI, region of interest.

further studies. Moreover, Figure S1 demonstrates the cortex and striatum of the contralateral using a 5-pool Lorentzian fitting at $B_{1\text{-sat}}$ =1 μT. Figure S1E compares the raw Z-spectra, subtracted by the fitted water and MT effects, of the cortex and striatum of the contralateral to quantify the CEST effects. Decreased signals were observed in the striatum in comparison to the cortex.

In addition, *Figure 4* shows 8 maps in a representative normal rat brain and for all the 5 rats scanned 2 hours after the transient MCAO was induced. Figure S2 shows 2 maps: T_{2w} (Figure S2A) and ADC (Figure S2B). The map results indicate that there was contrast between the two hemispheres of the normal control rat in ADC, T_{2w}, and the different quantification images, and that pixel-by-pixel fitted quantification images using the MTR_{asym} and MTR_{Rex} also did not reveal a contrast between the lesion hemisphere

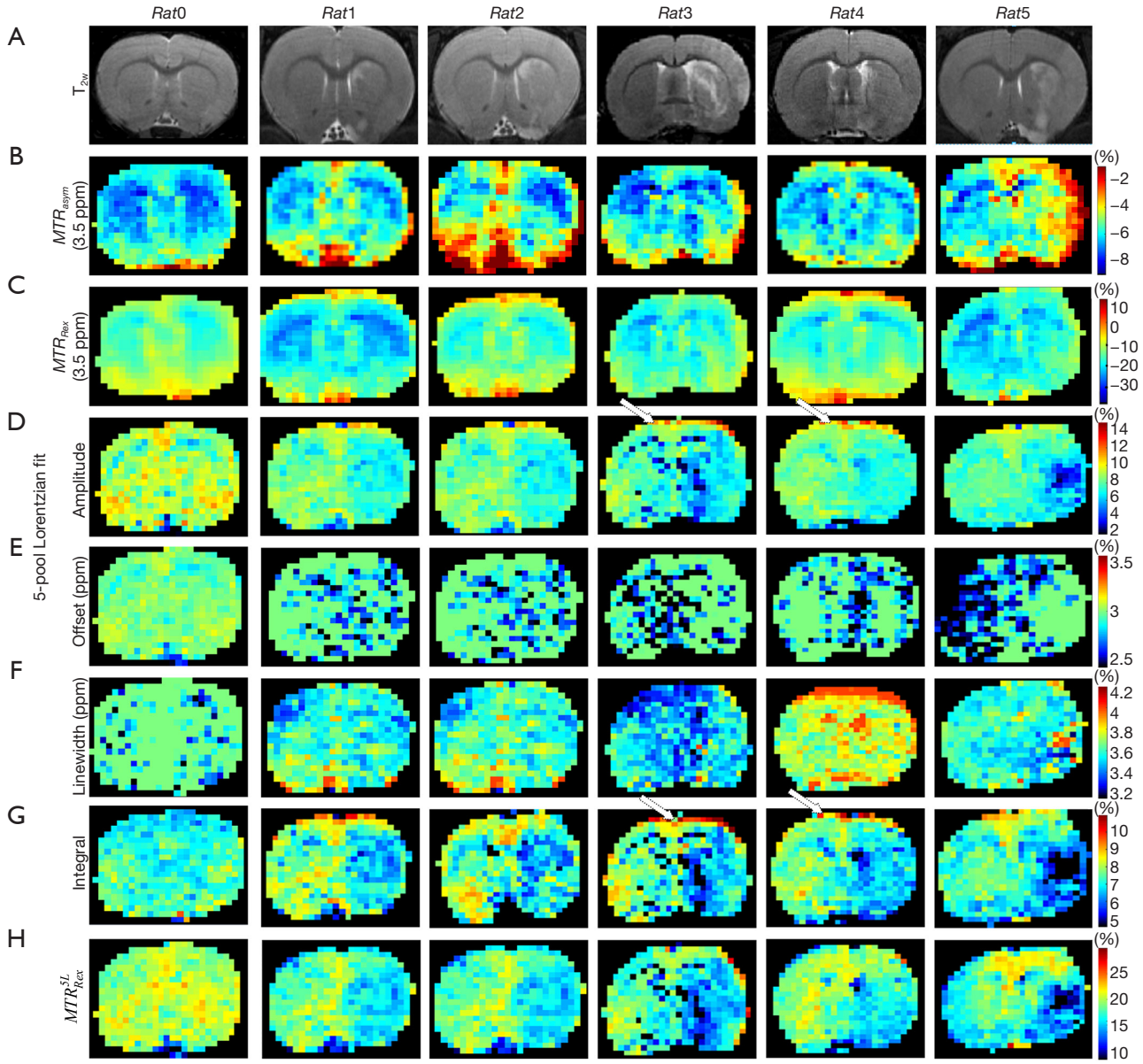

Figure 4 The multiparametric maps used in this study. (A) T_2-weighted images and contrast maps at 3.5 ppm using a pixel-by-pixel amplitude fitted by (B) MTR_{asym} and (C) MTR_{Rex}. Contrast maps at 3.5 ppm using a pixel-by-pixel fitted (D) amplitude, (E) offset, (F) linewidth, and (G) integral using a 5-pool Lorentzian fitting. Pixel-by-pixel fitted amplitude maps of each pool using MTR_{Rex}^{5L} (H), at 3.5 ppm, in a representative normal rat brain (Rat0) and for all stroke rats (from Rat 1 to Rat 5). MTR_{asym}, magnetization transfer ratio based on asymmetry; MTR_{Rex}, spillover-corrected magnetization transfer ratio yielding rex; MTR_{Rex}^{5L}, combined 5-pool Lorentzian fitting and reciprocal of Z-spectra.

and contralateral hemisphere. The amplitude, integral using a 5-pool Lorentzian fitting, MTR_{Rex}^{5L}, and the ADC, all exhibited obvious hypointensity at the lesion hemisphere. However, the amplitude and the integral using a 5-pool Lorentzian fitting exhibited unexpectedly high signals, as indicated by the white arrow. Moreover, as a comparison method, MTR_{Rex}^{5L} and MTR_{Rex}^{VOPVP} have been added. The results are displayed in Figure S3.

Table 2 summarizes the data of the CNR of images of the individual rats (n=5) after 2 hours of the transient MCAO induction, in which the results of stroke lesion regions and the contralateral side are in a matrix of 4×4 pixels. A higher

Table 2 Differences in CNR between a 5-pool Lorentzian fit and MTR_{Rex}^{5L} of contralateral normal and stroke lesion tissue at $B_{1\text{-sat}}$ =1 μT

Rat #	Method	APT (3.5 ppm)
Rat 1	MTR_{Rex}^{VOPVP}	3.20
	5-pool Lorentzian fit (integral)	3.05
	MTR_{Rex}^{5L}	3.19
Rat 2	MTR_{Rex}^{VOPVP}	3.67
	5-pool Lorentzian fit (integral)	3.31
	MTR_{Rex}^{5L}	3.83
Rat 3	MTR_{Rex}^{VOPVP}	4.57
	5-pool Lorentzian fit (integral)	3.32
	MTR_{Rex}^{5L}	3.93
Rat 4	MTR_{Rex}^{VOPVP}	2.53
	5-pool Lorentzian fit (integral)	2.98
	MTR_{Rex}^{5L}	3.32
Rat 5	MTR_{Rex}^{VOPVP}	3.41
	5-pool Lorentzian fit (integral)	4.32
	MTR_{Rex}^{5L}	4.87
Average	MTR_{Rex}^{VOPVP}	3.48
	5-pool Lorentzian fit (integral)	3.40
	MTR_{Rex}^{5L}	3.83

CNR, contrast-to-noise ratio; APT, amide proton transfer; MTR_{Rex}^{5L}, combined 5-pool Lorentzian fitting and reciprocal of Z-spectra; MTR_{Rex}^{VOPVP}, combined Voxel-wise optimization pseudo Voigt profile and reciprocal of Z-spectra.

CNR was obtained by the MTR_{Rex}^{5L} method in comparison to both the MTR_{Rex}^{VOPVP} and a 5-pool Lorentzian fitting (12). Notably, at 3.5 ppm, MTR_{Rex}^{5L} obtained the highest average CNR (~3.83); this exceeded the MTR_{Rex}^{VOPVP} (~3.48) and 5-pool Lorentzian fitting (integral) (~3.40).

Figure 5 shows the fitted amplitude maps of each pool with a 5-pool Lorentzian fit in a representative normal rat (*Figure 5A*) and for all stroke rats (*Figure 5B*). The images of MT, water, and NOE did not reveal a contrast between the 2 hemispheres in a normal control rat and all of the stroke rats. However, the amplitude using a 5-pool Lorentzian fitting at 2 ppm exhibited an obvious hypointensity at the lesion hemisphere for Rat 1, Rat 2, and Rat 5. These results are consistent with previous findings (21).

Figure 6, Figure S4, and Figure S5 show the images of a representative rat brain at the time points 2, 6, and 24 hours after transient ischemia. As shown by the rat in *Figure 4*, T2w, ADC (Figure S5), and pixel-by-pixel fitted quantification images using the MTR_{asym} and MTR_{Rex} did not reveal a contrast between the lesion hemisphere and contralateral hemisphere. In contrast, the pixel-by-pixel fitted amplitude and the integral using a 5-pool Lorentzian fitting exhibit unexpectedly high signals, as indicated by the white arrow (*Figure 4*). At later points in time, these high signals gradually became less apparent; in addition, the contrast involved over time.

The contribution of the composition from each pool observed in the MTR_{Rex}^{VOPVP} was further evaluated. The fitted amplitude, offset, linewidth, and integral maps of each pool using a 5-pool Lorentzian fitting, and the fitted amplitude of each pool using MTR_{Rex}^{5L}, were performed on each fitted pool. *Figure 7* compares the signals between the contralateral and the stroke lesion regions of each pool with bar plots for 4 representative rat brains with stroke. The results indicated there were 2 cases without substantial differences between the 2 hemispheres in the fitted offset of each pool. The first case used offset maps of each pool using 5-pool Lorentzian fitting (*Figure 7B*), and the second used linewidth maps of each pool except with a fitted water pool using 5-pool Lorentzian fitting (*Figure 7C*). The results indicated there were 3 cases with more substantial differences. First, the amplitude of the fitted amplitude using a 5-pool Lorentzian fitting of MT at –2 ppm (23.25%±1.66%; 11.95%±2.06%) and amide at 3.5 ppm (6.04%±0.39%; 6.86%±0.39%) was decreased in a stroke lesion in comparison to the contralateral normal tissue (*Figure 7A*). Second, the difference of fitted integral amplitude using a 5-pool Lorentzian fitting of MT at –2 ppm (23.22%±4.10%; 11.952%±4.60%) and amide at 3.5 ppm (6.00%±0.98%; 6.82%±0.87%) was also decreased between a stroke lesion and the contralateral normal tissue (*Figure 7D*). Third, compared with the value of 15.69%±1.99% of the contralateral normal tissue, the amplitude of MTR_{Rex}^{5L} of amide at 3.5 ppm in a stroke lesion decreased to 13.83%±2.20% (*Figure 7E*).

Discussion

In this study, a CEST quantitative method, namely MTR_{Rex}^{5L}, was used by subtracting the inverse Z-spectra from the Z-spectra with the fitted reference spectrum using a 5-pool

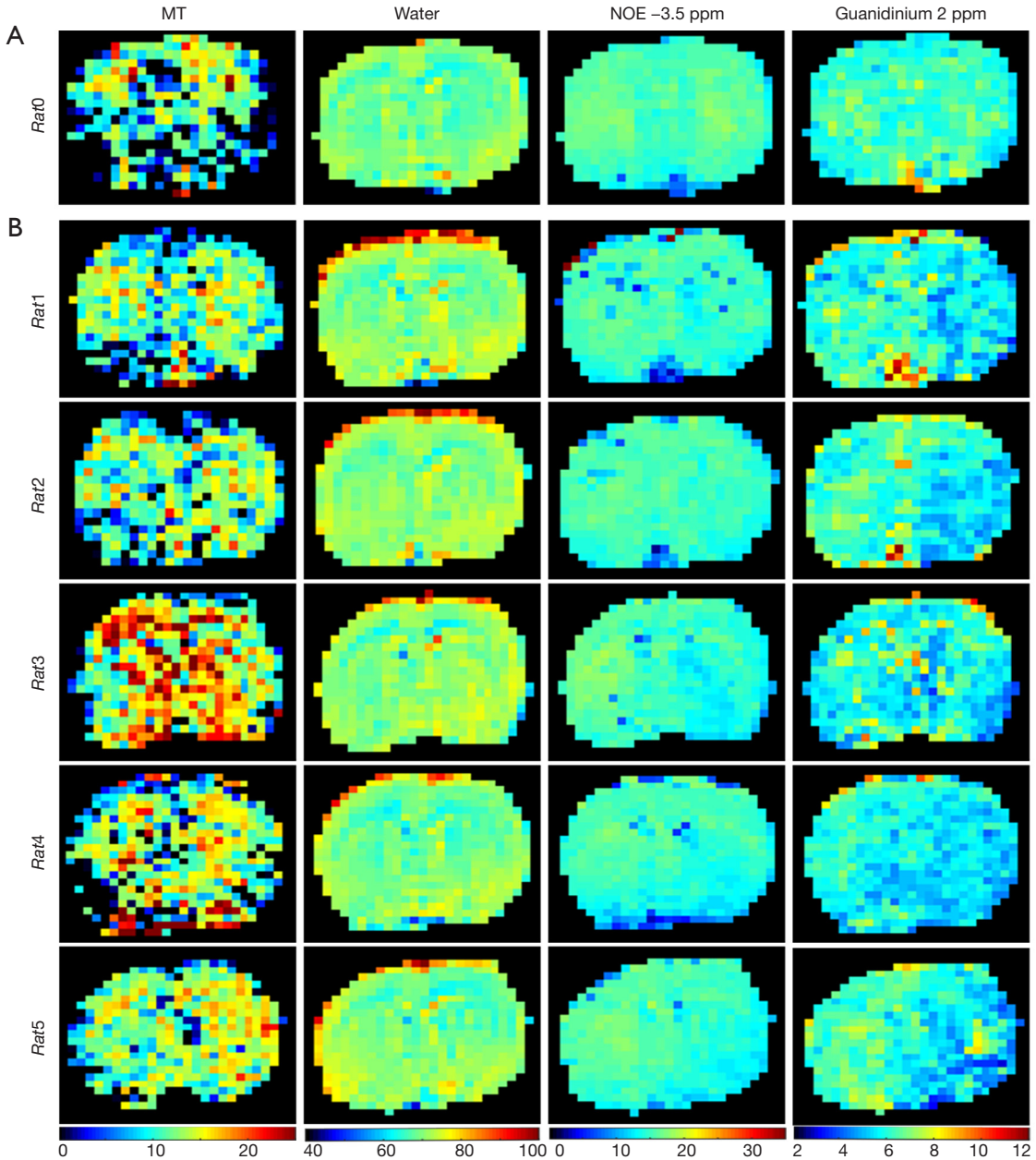

Figure 5 Fitted amplitude maps of each pool using a 5-pool Lorentzian fit (A) in a representative normal rat and (B) for all stroke rats (from Rat 1 to Rat 5). MT, magnetization transfer; NOE, nuclear Overhauser enhancement.

Lorentzian fitting to detect tissue acidosis following an acute stroke. The fitted amplitude maps from the MTR_{Rex}^{5L} approach revealed smaller amide effects in the ipsilateral striatum than those in the contralateral striatum. These results are similar to the previous findings using a 5-pool Lorentzian Z-spectral fitting (33) and the MTR_{Rex}^{VOPVP} method (12). Previous studies have shown that the effect of APT may reduce owing to a drop in tissue pH values during MCAO (11). Research also indicates that the MTR_{Rex}^{VOPVP} method, by subtracting the inverse Z-spectra from the Z-spectra with the fitted reference spectra using VOPVP, could detect an ischemic stroke (12). It another study, the changes in the MTR_{asym} contrast were predominantly attributable to APT (3.5 ppm) effects during acute ischemia under a multi-pool Lorentzian

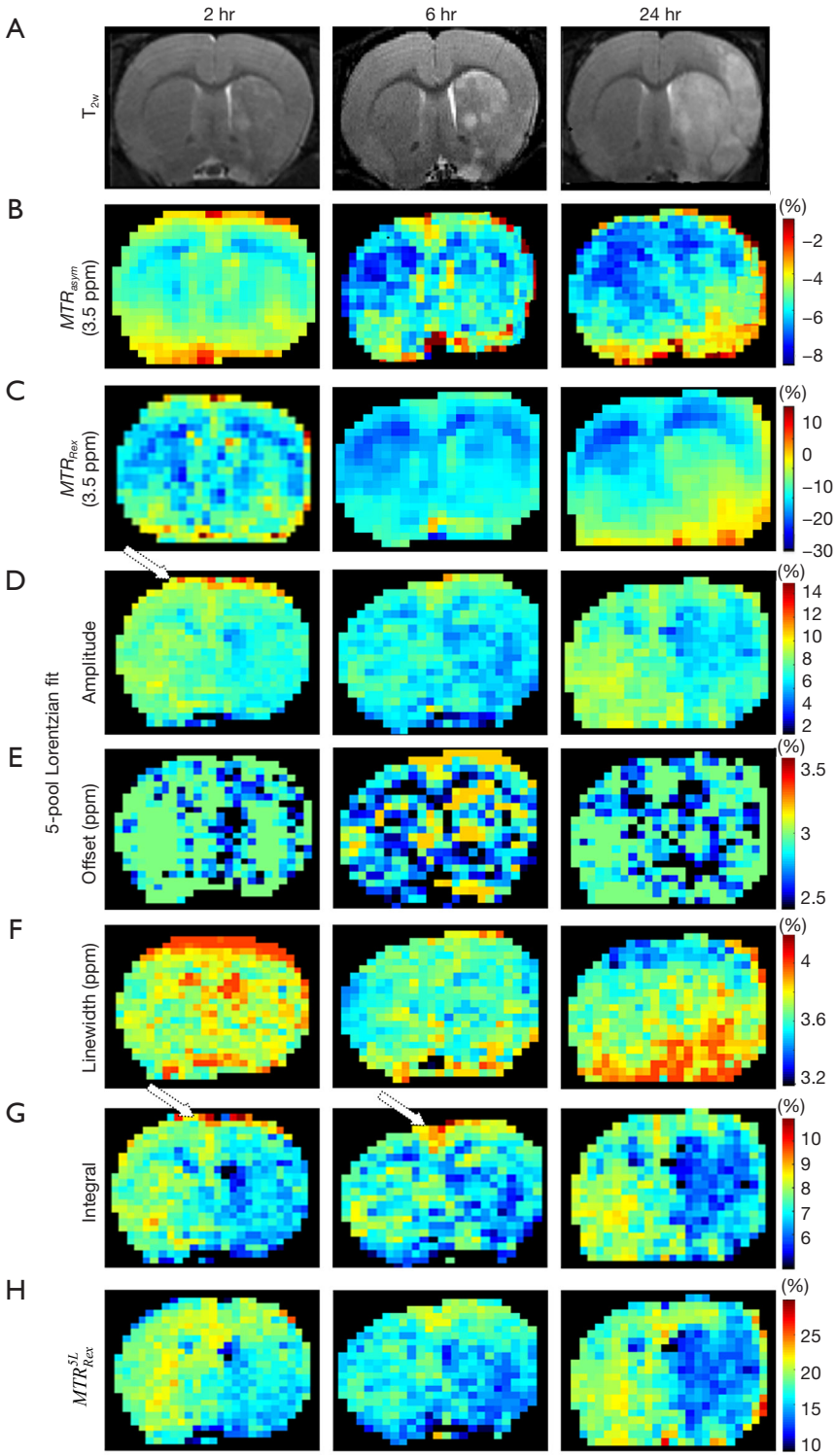

Figure 6 The multiparametric maps used in this study. (A) T_2-weighted, pixel-by-pixel fitted amplitude using (B) MTR_{asym} and (C) MTR_{Rex}. Pixel-by-pixel fitted (D) amplitude, (E) offset, (F) linewidth, and (G) integral using 5-pool Lorentzian fit. Pixel-by-pixel fitted amplitude maps and (H), at 3.5 ppm at different times after a stroke from a representative rat. MTR_{asym}, magnetization transfer ratio based on asymmetry; MTR_{Rex}, spillover-corrected magnetization transfer ratio yielding rex.

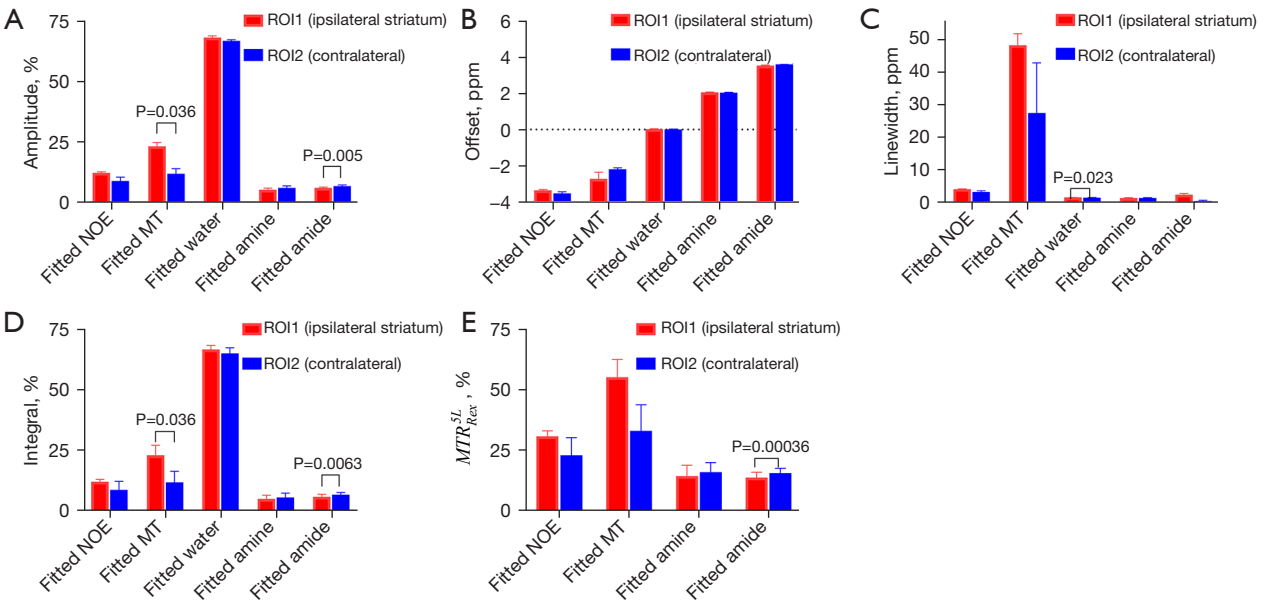

Figure 7 The statistical analysis of the fitted parameters in this study. (A) Amplitude, (B) offset, (C) linewidth, and (D) integral maps of each pool using 5-pool Lorentzian fit, and (E) amplitude of each pool using MTR_{Rex}^{5L}, in a representative rat brain with a stroke. ROI, region of interest; MT, magnetization transfer; NOE, nuclear Overhauser enhancement; MTR_{Rex}^{5L}, combined 5-pool Lorentzian fitting and reciprocal of Z-spectra.

fitting (21), which is consistent with previous findings (8). In our study, the fitted line width maps from the 5-pool Lorentzian fit approach revealed higher DS effects in the ipsilateral striatum than those in the contralateral striatum (*Figure 7*). The MTR_{Rex}^{5L} method permitted us to isolate these effects using pool modeling systems and enabled us to determine their specific contributions. Furthermore, at 3.5 ppm, MTR_{Rex}^{5L} obtained the highest average CNR in comparison to both MTR_{Rex}^{VOPVP} and a 5-pool Lorentzian fitting.

The inverse of the Z-spectrum and combinations of the inverse Z-spectrum with other quantization methods represent recently developed approaches. Reports show that a magnetization transfer ratio (MTR_{Rex}) based on the inverse Z-spectrum is helpful in the quantification of CEST-MRI evaluation of stroke lesions (11). Studies have used the three-offset (17) and the VOPVP as the reference signal (15). A study using a similar fitting method to the one proposed here demonstrated that a new NOE-mediated MT signal at approximately –1.6 ppm could be detected reliably. Both these fitting methods share a common feature: the –1.6 ppm dips and the dip after a stroke are very small. A recent comparative study reported that a multi-pool Lorentzian fitting offered a more accurate quantification of the CEST effects (22), especially at low irradiation, which may be underestimated by the three-offset method and overestimated by the LD. Traditionally, the difference between the Z-reference and the Z-spectrum (Z-residual) has been used to reduce the effects of DS (33). However, the Z-residual cannot completely eliminate the DS effect (23). There are two possible reasons for combining a multi-pool Lorentzian fitting and an inverse Z-spectra. First, it can eliminate all known competitive effects, comprising MT, NOE (–3.5 ppm), and DS. Second, it can amplify the small dips, which can enhance the sensitivity of the detection.

It has been reported that there is a significant signal reduction in the CEST effect at 3.5 ppm for ischemia detection, which is consistent with previously reported results (12). *Figure 1* shows that the Z-spectrum obtained from the experimental data was different from the simulation that used the tissue parameters listed in *Table 1*, especially when the frequency deviation was in the range of –1 to –2 ppm. The possible reason for this is that there is –1.6 ppm in the real Z-spectrum data, but this pool was not added in the simulation (23). As a result, the accuracy of the fitting and the number of fitting parameters were compromised.

Evaluations of parameters that may be used as a marker for detecting an acute ischemic stroke were proposed in previous research (33). In this work, we demonstrated that

the fitted amplitude using a 5-pool Lorentzian fitting of MT at –2 ppm and amide at 3.5 ppm, the amplitude of the fitted integral using a 5-pool Lorentzian fitting of MT at –2 ppm and amide at 3.5 ppm, and the amplitude using amide at 3.5 ppm may be used as a marker for detection of acute ischemic stroke at an early stage.

The CEST signal at 2 ppm is considered to be in the intermediate exchange regime. Thus, it is expected to increase with decreasing pH and show hyperintensity in stroke lesions. However, in our study, the Lorentzian fitting at 2 ppm showed hypointensity at the lesion for 3 rats, but not all rats (*Figure 5*), which is consistent with previously reported results (34). The reason for this conflicting result for the CEST signal at 2 ppm is that the multiple-pool Lorentzian fit of the amine CEST effect at 2 ppm has contributions from both the arginine amine and the fast exchanging pools, which change in the opposite direction during ischemic stroke. This leads to an insignificant correlation of the Lorentzian fit of amine CEST effects with APT and the varying results in different experimental conditions reported previously (34).

Conclusions

In conclusion, CEST-MRI with a quantitative MTR_{Rex}^{5L} may enhance the detection of ischemic stroke.

Acknowledgments

The authors would like to thank Dr. Xiaolei Song for the helpful discussions and EditSprings (https://www.editsprings.cn) for the expert linguistic services provided.
Funding: This work was supported by the Doctor Fund Project of Henan Polytechnic University (No. B2022-11), the Fundamental Research Funds for the Universities of Henan Province (No. NSFRF220407), and the Science and Technology Research of Henan Province (No. 212102310084).

Footnote

Conflicts of Interest: All authors have completed the ICMJE uniform disclosure form (available at https://qims.amegroups.com/article/view/10.21037/qims-22-420/coif). The authors have no conflicts of interest to declare.

Ethical Statement: The authors are accountable for all aspects of the work in ensuring that questions related to the accuracy or integrity of any part of the work are appropriately investigated and resolved. This study was approved by the ethics board of Weifang Medical University in compliance with institutional guidelines for the care and use of animals.

References

1. Zhou J, Payen JF, Wilson DA, Traystman RJ, van Zijl PC. Using the amide proton signals of intracellular proteins and peptides to detect pH effects in MRI. Nat Med 2003;9:1085-90.
2. Sun PZ, Zhou J, Sun W, Huang J, van Zijl PC. Detection of the ischemic penumbra using pH-weighted MRI. J Cereb Blood Flow Metab 2007;27:1129-36.
3. Msayib Y, Harston GWJ, Tee YK, Sheerin F, Blockley NP, Okell TW, Jezzard P, Kennedy J, Chappell MA. Quantitative CEST imaging of amide proton transfer in acute ischaemic stroke. Neuroimage Clin 2019;23:101833.
4. Zu Z, Afzal A, Li H, Xie J, Gore JC. Spin-lock imaging of early tissue pH changes in ischemic rat brain. NMR Biomed 2018;31:e3893.
5. Wang E, Wu Y, Cheung JS, Igarashi T, Wu L, Zhang X, Sun PZ. Mapping tissue pH in an experimental model of acute stroke - Determination of graded regional tissue pH changes with non-invasive quantitative amide proton transfer MRI. Neuroimage 2019;191:610-7.
6. Heo HY, Zhang Y, Jiang S, Lee DH, Zhou J. Quantitative assessment of amide proton transfer (APT) and nuclear overhauser enhancement (NOE) imaging with extrapolated semisolid magnetization transfer reference (EMR) signals: II. Comparison of three EMR models and application to human brain glioma at 3 Tesla. Magn Reson Med 2016;75:1630-9.
7. Bie C, Liang Y, Zhang L, Zhao Y, Chen Y, Zhang X, He X, Song X. Motion correction of chemical exchange saturation transfer MRI series using robust principal component analysis (RPCA) and PCA. Quant Imaging

Med Surg 2019;9:1697-713.
8. Zhou IY, Lu D, Ji Y, Wu L, Wang E, Cheung JS, Zhang XA, Sun PZ. Determination of multipool contributions to endogenous amide proton transfer effects in global ischemia with high spectral resolution in vivo chemical exchange saturation transfer MRI. Magn Reson Med 2019;81:645-52.
9. Zhou J, van Zijl PCM. Chemical exchange saturation transfer imaging and spectroscopy. Progress in Nuclear Magnetic Resonance Spectroscopy, 2006;48:109-36.
10. Jin T, Wang P, Zong X, Kim SG. Magnetic resonance imaging of the Amine-Proton EXchange (APEX) dependent contrast. Neuroimage 2012;59:1218-27.
11. Zaiss M, Xu J, Goerke S, Khan IS, Singer RJ, Gore JC, Gochberg DF, Bachert P. Inverse Z-spectrum analysis for spillover-, MT-, and T1 -corrected steady-state pulsed CEST-MRI--application to pH-weighted MRI of acute stroke. NMR Biomed 2014;27:240-52.
12. Zhang L, Liang Y, Chen Y, Li G, Zhang M, Zhao Y, Wang X, Song X. Enhanced CEST MRI Using the Residual of Inversed Z-Spectra for Ischemia Detection. IEEE Access, 2020;8:147323-36.
13. Msayib Y, Harston GWJ, Sheerin F, Blockley NP, Okell TW, Jezzard P, Kennedy J, Chappell MA. Partial volume correction for quantitative CEST imaging of acute ischemic stroke. Magn Reson Med 2019;82:1920-8.
14. Song X, Gilad AA, Joel S, Liu G, Bar-Shir A, Liang Y, Gorelik M, Pekar JJ, van Zijl PC, Bulte JW, McMahon MT. CEST phase mapping using a length and offset varied saturation (LOVARS) scheme. Magn Reson Med 2012;68:1074-86.
15. Zhang L, Zhao Y, Chen Y, Bie C, Liang Y, He X, Song X. Voxel-wise Optimization of Pseudo Voigt Profile (VOPVP) for Z-spectra fitting in chemical exchange saturation transfer (CEST) MRI. Quant Imaging Med Surg 2019;9:1714-30.
16. Tietze A, Blicher J, Mikkelsen IK, Østergaard L, Strother MK, Smith SA, Donahue MJ. Assessment of ischemic penumbra in patients with hyperacute stroke using amide proton transfer (APT) chemical exchange saturation transfer (CEST) MRI. NMR Biomed 2014;27:163-74.
17. Jin T, Wang P, Zong X, Kim SG. MR imaging of the amide-proton transfer effect and the pH-insensitive nuclear overhauser effect at 9.4 T. Magn Reson Med 2013;69:760-70.
18. Zhou IY, Wang E, Cheung JS, Zhang X, Fulci G, Sun PZ. Quantitative chemical exchange saturation transfer (CEST) MRI of glioma using Image Downsampling Expedited Adaptive Least-squares (IDEAL) fitting. Sci Rep 2017;7:84.
19. Windschuh J, Zaiss M, Meissner JE, Paech D, Radbruch A, Ladd ME, Bachert P. Correction of B1-inhomogeneities for relaxation-compensated CEST imaging at 7 T. NMR Biomed 2015;28:529-37.
20. Cai K, Singh A, Poptani H, Li W, Yang S, Lu Y, Hariharan H, Zhou XJ, Reddy R. CEST signal at 2ppm (CEST@2ppm) from Z-spectral fitting correlates with creatine distribution in brain tumor. NMR Biomed 2015;28:1-8.
21. Wu Y, Zhou IY, Lu D, Manderville E, Lo EH, Zheng H, Sun PZ. pH-sensitive amide proton transfer effect dominates the magnetization transfer asymmetry contrast during acute ischemia-quantification of multipool contribution to in vivo CEST MRI. Magn Reson Med 2018;79:1602-8.
22. Zhang XY, Wang F, Li H, Xu J, Gochberg DF, Gore JC, Zu Z. Accuracy in the quantification of chemical exchange saturation transfer (CEST) and relayed nuclear Overhauser enhancement (rNOE) saturation transfer effects. NMR Biomed 2017;30:10.1002/nbm.3716.
23. Zhang XY, Wang F, Jin T, Xu J, Xie J, Gochberg DF, Gore JC, Zu Z. MR imaging of a novel NOE-mediated magnetization transfer with water in rat brain at 9.4 T. Magn Reson Med 2017;78:588-97.
24. Woessner DE, Zhang S, Merritt ME, Sherry AD. Numerical solution of the Bloch equations provides insights into the optimum design of PARACEST agents for MRI. Magn Reson Med 2005;53:790-9.
25. Heo HY, Lee DH, Zhang Y, Zhao X, Jiang S, Chen M, Zhou J. Insight into the quantitative metrics of chemical exchange saturation transfer (CEST) imaging. Magn Reson Med 2017;77:1853-65.
26. Zaiss M, Zu Z, Xu J, Schuenke P, Gochberg DF, Gore JC, Ladd ME, Bachert P. A combined analytical solution for chemical exchange saturation transfer and semi-solid magnetization transfer. NMR Biomed 2015;28:217-30.
27. Liu H, Jablonska A, Li Y, Cao S, Liu D, Chen H, Van Zijl PC, Bulte JW, Janowski M, Walczak P, Liu G. Label-free CEST MRI Detection of Citicoline-Liposome Drug Delivery in Ischemic Stroke. Theranostics 2016;6:1588-600.
28. Kim M, Gillen J, Landman BA, Zhou J, van Zijl PC. Water saturation shift referencing (WASSR) for chemical exchange saturation transfer (CEST) experiments. Magn Reson Med 2009;61:1441-50.
29. Zaiss M. cest-sources. Available online: https://github.

com/cest-sources/Z-cw
30. Zhao Y, Chen Y, Chen Y, Zhang L, Wang X, He X. A fully convolutional network (FCN) based automated ischemic stroke segment method using chemical exchange saturation transfer imaging. Med Phys 2022;49:1635-47.
31. Heo HY, Zhang Y, Burton TM, Jiang S, Zhao Y, van Zijl PCM, Leigh R, Zhou J. Improving the detection sensitivity of pH-weighted amide proton transfer MRI in acute stroke patients using extrapolated semisolid magnetization transfer reference signals. Magn Reson Med 2017;78:871-80.
32. Li H, Zu Z, Zaiss M, Khan IS, Singer RJ, Gochberg DF, Bachert P, Gore JC, Xu J. Imaging of amide proton transfer and nuclear Overhauser enhancement in ischemic stroke with corrections for competing effects. NMR Biomed 2015;28:200-9.
33. Zhang XY, Wang F, Afzal A, Xu J, Gore JC, Gochberg DF, Zu Z. A new NOE-mediated MT signal at around -1.6ppm for detecting ischemic stroke in rat brain. Magn Reson Imaging 2016;34:1100-6.
34. Cui J, Afzal A, Zu Z. Comparative evaluation of polynomial and Lorentzian lineshape-fitted amine CEST imaging in acute ischemic stroke. Magn Reson Med 2022;87:837-49.

Cite this article as: Zhang L, Xu C, Li Z, Sun J, Wang X, Hou B, Zhao Y. Chemical exchange saturation transfer (CEST) magnetic resonance imaging (MRI) quantification of transient ischemia using a combination method of 5-pool Lorentzian fitting and inverse Z-spectrum analysis. Quant Imaging Med Surg 2023;13(3):1860-1873. doi: 10.21037/qims-22-420

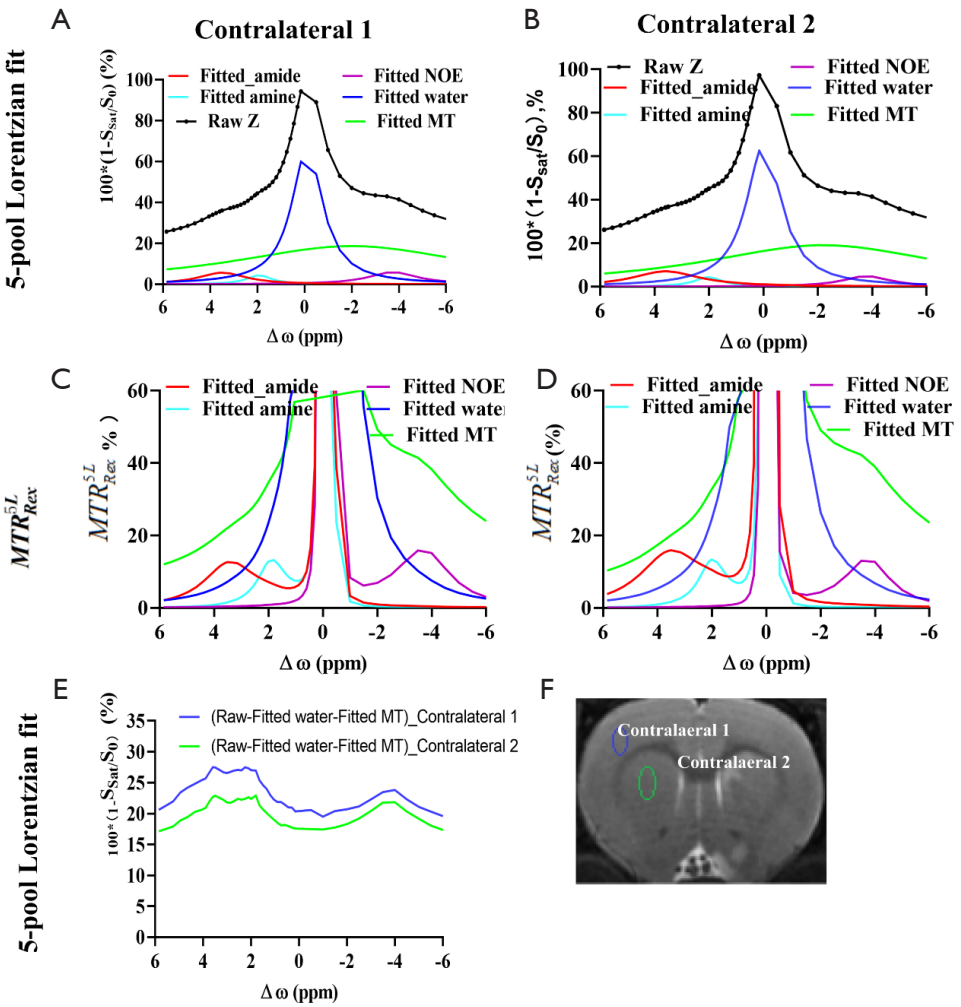

Figure S1 The spectra analysis between ipsilateral striatum (left column) and contralateral (right column). (A,B) A 5-pool Lorentzian fitting of Z-spectra from contralateral 1 and contralateral 2, the top panel, including saturation transfer from-3.5, 2, 3.5 ppm as direct saturation and MT contributions. (C,D) The bottom panels are MTR_{Rex}^{5L} from contralateral 1 (cortex) and contralateral 2 (striatum). (E) The fitted water and MT effects are subtracted from the raw Z-spectra, showing apparent CEST contrast between contralateral 1 and contralateral 2 tissues at amide (3.5 ppm) and guanidinium (2 ppm). (F) The T_{2w} image marked with a contralateral 1ROI and contralateral 2 (striatum) ROI a for spectral analysis. NOE, nuclear Overhauser enhancement, MT, magnetization transfer; CEST, chemical exchange saturation transfer; ROI, region of interest.

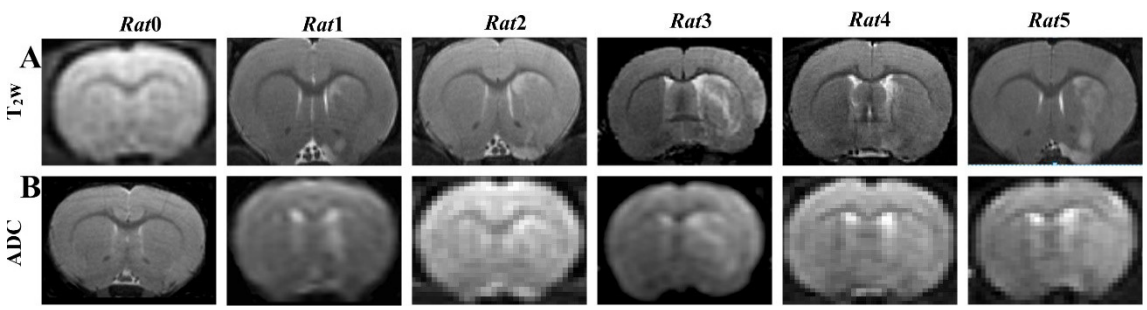

Figure S2 Multi-parametric maps used in this study. (A) T_{2w} (B) ADC, in a representative normal rat brain (Rat0) and for all stroke rats (from Rat1 to Rat5). ADC, apparent diffusion coefficient.

https://dx.doi.org/10.21037/qims-22-420

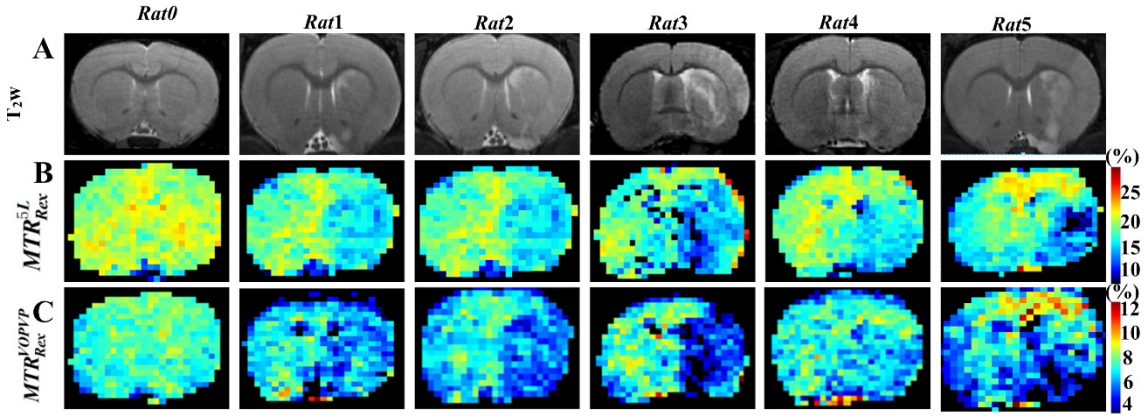

Figure S3 Multi-parametric maps used in this study. (A) T_{2w} as well as contrast maps at 3.5 ppm using a pixel-by-pixel fitted by (B) MTR_{Rex}^{5L}, (C) MTR_{Rex}^{VOPVP}, at 3.5 ppm, in a representative normal rat brain (Rat0) and for all stroke rats (from Rat1 to Rat5).

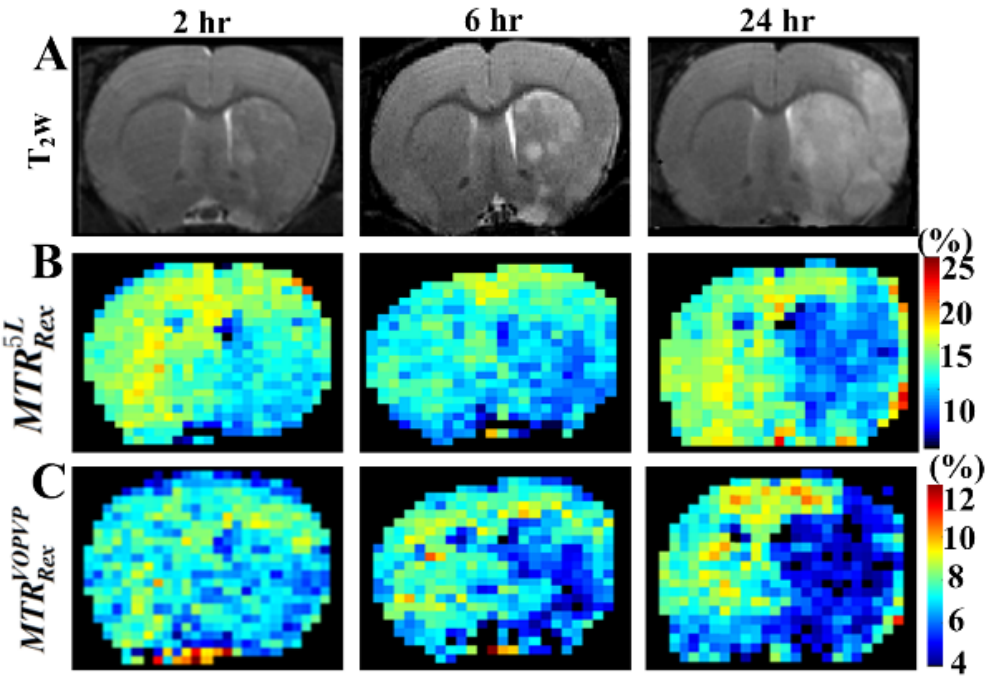

Figure S4 Multi-parametric maps used in this study. (A) T_{2w}, pixel-by-pixel fitted using (B) MTR_{Rex}^{5L}, (C) MTR_{Rex}^{VOPVP}, at 3.5 ppm at different times after a stroke from a representative rat.

https://dx.doi.org/10.21037/qims-22-420

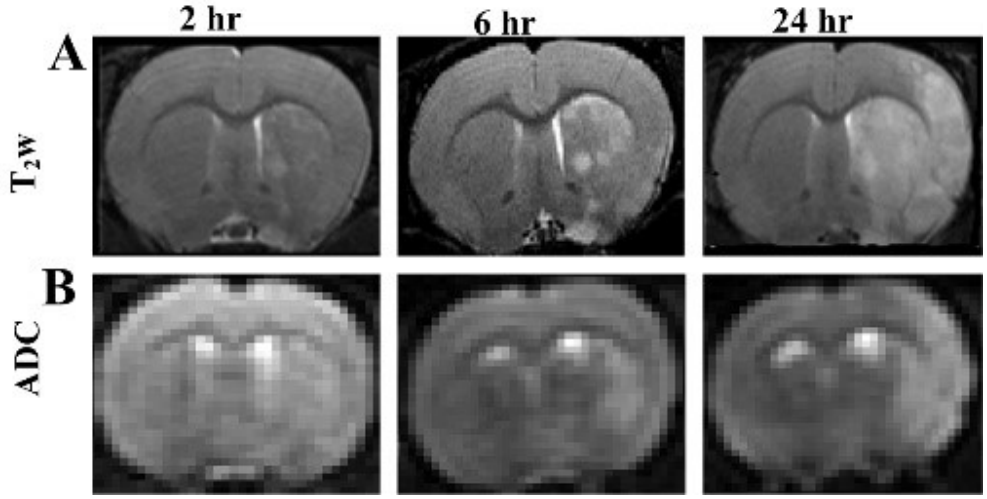

Figure S5 Multi-parametric maps used in this study. (A) T_{2w}, (B) ADC at different times after a stroke from a representative rat. ADC, apparent diffusion coefficient.

https://dx.doi.org/10.21037/qims-22-420